Quantum kinetic theory model of a continuous atom laser

G. R. Dennis,[1] Matthew J. Davis,[2] and J. J. Hope[1,*]

[1]*Department of Quantum Science, ARC Centre of Excellence for Quantum-Atom Optics, Australian National University, Canberra, ACT 0200, Australia*

[2]*School of Mathematics and Physics, ARC Centre of Excellence for Quantum-Atom Optics, The University of Queensland, Brisbane, QLD 4072, Australia*

(Received 4 May 2012; published 26 July 2012)

We investigate the feasible limits for realizing a continuously evaporated atom laser with high-temperature sources. A plausible scheme for realizing a truly continuous atom laser is to outcouple atoms from a partially condensed Bose gas while continuously reloading the system with noncondensed thermal atoms and performing evaporative cooling. Here we use quantum kinetic theory to model this system and estimate feasible limits for the operation of such a scheme. For sufficiently high temperatures, the figure of merit for the source is shown to be the phase-space flux. The dominant process limiting the usage of sources with low phase-space flux is the three-body loss of the condensed gas. We conclude that certain double-magneto-optical trap sources may produce substantial mean condensate numbers through continuous evaporation and provide an atom laser source with a narrow linewidth and reasonable flux.

DOI: 10.1103/PhysRevA.86.013640 PACS number(s): 03.75.Kk, 03.75.Pp, 37.10.De

I. INTRODUCTION

The experimental realization of Bose-Einstein condensation (BEC) in dilute alkali-metal gases [1] has opened up the study of the atom laser: a coherent beam of atoms analogous to the optical laser. Like optical lasers, it is hoped that these atomic sources will demonstrate mode selectivity and high spectral flux [2]. The simplest method of producing a spatially coherent atomic beam is to couple atoms out of a trapped BEC [3]. Rapid outcoupling of a BEC forms a coherent atomic beam with a spread in momentum as large as the trapped BEC, whereas coupling the atoms out more slowly reduces the output linewidth at the expense of reducing the overall flux [4]. These atom lasers are equivalent to Q-switched optical lasers, which do not exhibit gain narrowing. Continuously pumping the atom laser to produce a stable output provides the obvious benefit of higher flux but may also improve the stability and linewidth of the output beam. In a gain-narrowed optical laser, a higher pumping rate both increases the total flux and reduces the linewidth of the output, producing a dramatically increased spectral flux [5]. An atom laser with gain narrowing must have a saturable, Bose-enhanced pumping mechanism that operates simultaneously with the damping [2]. This paper examines the limits on thermal sources that can be used to produce a continuous atom laser through the process of continuous evaporation.

The two essential steps towards providing a continuous pumping mechanism for an atom laser are (1) the provision of atoms from an external source to the atomic trap and (2) a process that causes at least some of those atoms to make an irreversible, stimulated transition into the BEC. Continuous delivery of ultracold atoms has been demonstrated in a number of experiments [6–9] and is an important component of thermal atomic interferometry. Sequential reloading of a target BEC was achieved using optical tweezers [6], where a series of source condensates were joined by manipulating the trapping potentials, and excitations were subsequently removed by further evaporative cooling. This milestone experiment maintained the condensate fraction and, therefore, the flux of a potential atom laser. However, an atom laser produced from such an experiment would not possess the desired narrow linewidth, as merging two coherent sources by manipulating the potential is not a Bose-enhanced process. This means that the phase of the lasing mode would diffuse at a rate proportional to the replenishment rate. In this paper it is shown that, under certain conditions, a similar experiment using an ultracold *thermal* source would be able to pump the target BEC and maintain a significant BEC population using a phase-preserving Bose-enhanced scattering process.

Atom-stimulated transitions into the condensate can be made irreversible by coupling to a reservoir. There are two possible reservoirs: the empty modes of the electromagnetic field accessible via a transition from an excited atomic state (as used in optical cooling), or the empty modes of the atomic field (accessible via evaporation). Optical cooling is an obvious candidate for a continuous process, but it has not yet achieved BEC. This is because condensates are very sensitive to the resonant light that is emitted by the spontaneous emission step in the cooling, as the recoil energy of a single photon is significantly larger than the energy per particle. Several early atom laser models were based on optical cooling from a thermal source [10], but they have not been experimentally realized. The only optical cooling method that has led to an increase in BEC number required a precondensed source in the same trap [11].

The last stage of cooling for production of all current BECs from thermal sources has been mediated by atom-atom interactions. This has the advantage that it can be performed without the presence of resonant light, but the obvious disadvantage is that it relies on the system approaching thermal equilibrium and will therefore be reversed by the addition of atoms above the condensation temperature. However, if the atoms can be supplied at the same time that the system undergoes a forced evaporation process, then, even if the source atoms are above the condensation temperature, it is possible under some conditions to produce a net gain for the

*joseph.hope@anu.edu.au

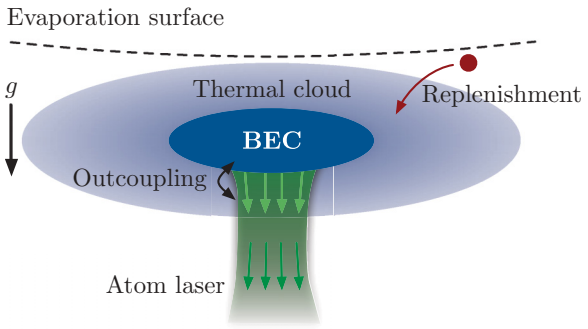

FIG. 1. (Color online) Schematic of the experimental setup.

condensate mode. It is therefore plausible to make evaporative cooling operate in a continuous fashion. While progress has been made towards implementing such a continuous atom delivery scheme [12], we do not examine the details of the delivery of thermal atoms. The focus of this investigation is to determine exactly what the requirements are for a thermal source to produce a continuously replenished BEC.

The quantum kinetic theory of dilute gas BEC has been successfully used to model condensate growth [13,14]. We extend this model to include loss due to three-body inelastic scattering, which turns out to be a key determinant of the required phase-space flux required in the thermal source. In Sec. II, we describe the schematic of our proposed pumping scheme, and the details of the quantum kinetic theory model are discussed in Sec. III. The results of the model are examined in Sec. IV.

II. ATOM LASER SCHEME

The proposed scheme for a pumped atom laser is illustrated in Fig. 1. It is very similar to the methods used to evaporate a thermal cloud to condensation in a magnetic trap and produce a (quasicontinuous) atom laser. In our scheme, the thermal cloud is continuously replenished by a process that couples it to a source of atoms at finite temperature. This coupling process is assumed to transfer atoms irreversibly from the source to the thermal cloud without changing their energy distribution. This process cannot be as simple as a repeated merging of traps, as this replenishment process results in a local entropy decrease that must be balanced by an entropy increase in some reservoir. An example of such a replenishment process has been demonstrated in Ref. [12], where atoms enter in an excited internal state and are optically pumped into the thermal cloud, carrying excess entropy in the emitted photons.

The gain process for the condensate is the same Bose-enhanced scattering between thermal atoms and the condensate that drives condensate growth when evaporating to produce BEC [13,15,16]. This process becomes irreversible when one of the scattered atoms has enough energy to cross the evaporation surface and be removed from the thermal cloud.

The atom laser beam itself is produced by large momentum-transfer Raman outcoupling from the condensate. Raman outcoupling improves the spatial properties of the beam [17] and allows minimal outcoupling from the thermal cloud when the two lasers are focused to intersect only in the immediate vicinity of the condensate.

A nonequilibrium steady state will be reached when the rate of atom loss from the condensate due to outcoupling balances the rate of atoms gained due to collisions within the thermal cloud. If the evaporative surface is tuned so that atoms of energy $\varepsilon_{\rm cut}$ and higher are rapidly and continually removed from the trap, then all collisions that result in an atom having energy greater than $\varepsilon_{\rm cut}$ will become irreversible. As $\varepsilon_{\rm cut}$ is lowered, a larger fraction of the scattering processes that leave atoms in the condensate mode will become irreversible. This suggests that there must be some value of $\varepsilon_{\rm cut}$ for which the condensate experiences net gain. What is not clear is whether the net gain can proceed efficiently, i.e., on a time scale much shorter than other losses from the condensate.

III. KINETIC THEORY MODEL

A. Model overview

Our model is an extension of the kinetic theory models described in [13,15], with the addition of three-body loss processes from both the condensate and the thermal cloud. This model was successfully used to study condensate formation experiments by Köhl *et al.* [18,19], Hugbart *et al.* [20], and Garrett *et al.* [21].

The starting point of the kinetic model is a separate treatment of the thermal and condensed components of the system. The condensed component is assumed to be a quantum fluid obeying a Gross-Pitaevskii-type equation; however, we make a further approximation and assume that the condensate is sufficiently occupied that it has a Thomas-Fermi profile [22], Chap. 6]. The condensate dynamics are then fully described by the number of condensed atoms $N_0(t)$.

We consider temperatures such that $k_B T \gg \mu$, such that the fraction of the thermal cloud that is phononlike is negligible. The thermal cloud is then described within the Hartree-Fock approximation [22, Chap. 8], which assumes the cloud is composed of particlelike excitations moving in the effective potential of the harmonic trap plus condensate mean field. We make a further approximation that we can treat the thermal cloud ergodically, i.e., that all points in the phase space having equal energy have equal population [23]. This is indeed a drastic approximation and is unlikely to be accurate in a realistic experiment, where evaporative cooling will almost certainly lead to a spatial dependence of the phase-space density. Unfortunately, it is computationally unfeasible to go beyond the ergodic approximation and directly solve the quantum Boltzmann equation. The only available option would be to use a Monte Carlo method (see, e.g., Ref. [24]). Additionally we note that several realistic experiments have been modeled within the ergodic approximation and in general have found excellent agreement with the experimental data [18–21]. Therefore, we strongly believe that there would be no qualitative and only a small quantitative change in our optimal evaporative cooling parameter were we to do this. Under these approximations, the thermal cloud is then described by its energy distribution function $g(\varepsilon,t)$ and the density of states, $\rho(\varepsilon,t)$.

As the model presented here is very similar to that presented in Ref. [13] with some additional terms, a derivation of the common terms is omitted. As a summary, the derivation proceeds by taking a semiclassical Boltzmann equation for

the phase-space distribution function of the thermal cloud, $f(\boldsymbol{r},\boldsymbol{p},t)$, including collisional terms and using the ergodic approximation to obtain an equation of motion for the energy distribution function $g(\varepsilon,t)$. This equation is self-consistently matched with a Gross-Pitaevskii equation for the condensate before making the Thomas-Fermi approximation to obtain an equation of motion for the number of condensed atoms, $N_0(t)$. An example application of this method to derive the appropriate terms for three-body loss is given in the Appendix. A detailed discussion of this theory is given in the review article [25].

B. Pumped atom laser equations of motion

Separating the contributions of the different processes involved, the equations of motion for the model for a collision-driven pumped atom laser considered here are

$$\begin{aligned}\frac{dN_0}{dt} &= \left.\frac{dN_0}{dt}\right|_{\text{thermal}-\text{condensate}} \\ &\quad + \left.\frac{dN_0}{dt}\right|_{3-\text{body loss}} \\ &\quad + \left.\frac{dN_0}{dt}\right|_{\text{outcoupling}},\end{aligned} \tag{1}$$

$$\begin{aligned}\frac{\partial(\rho g)}{\partial t} &= \left.\frac{\partial(\rho g)}{\partial t}\right|_{\text{thermal}-\text{thermal}} \\ &\quad + \left.\frac{\partial(\rho g)}{\partial t}\right|_{\text{thermal}-\text{condensate}} \\ &\quad + \left.\frac{\partial(\rho g)}{\partial t}\right|_{3-\text{body loss}} \\ &\quad + \left.\frac{\partial(\rho g)}{\partial t}\right|_{\text{replenishment}} \\ &\quad + \left.\frac{\partial(\rho g)}{\partial t}\right|_{\text{redistribution}},\end{aligned}$$

where the subscripts "thermal-thermal" and "thermal-condensate" denote Bose-enhanced collisional processes between atoms in the corresponding states [Figs. 2(a) and 2(b), respectively], the subscript "3-body loss" indicates the contribution due to three-body recombination, the subscript "replenishment" indicates the contribution due to the replenishment of the thermal cloud [Fig. 2(d)], the subscript "outcoupling" indicates the contribution due to outcoupling from the condensate to form the atom laser [Fig. 2(e)], and the subscript "redistribution" indicates the contribution due to the redistribution of population in energy space due to the changes of the energies of the occupied levels as the mean field of the condensate changes [Fig. 2(c)]. It is assumed that atoms with energy greater than the evaporative energy cutoff ε_{cut} are removed from the system sufficiently quickly such that $g(\varepsilon > \varepsilon_{\text{cut}}) = 0$.

1. The thermal cloud replenishment process

The thermal cloud is modeled as being continuously replenished from a source that provides a constant flux Φ of atoms at a temperature T. To avoid tying the model to any particular replenishment mechanism, we assume a best-case scenario in which each energy level ε in the source is coupled directly to the level in the thermal cloud with the same energy above the condensate chemical potential $\mu(t)$; i.e., the lowest energy level of the source ($\varepsilon = 0$) is coupled directly to the lowest energy level in the trap ($\varepsilon = \mu(t)$). This simple model gives the form of the contribution due to replenishment as

$$\left.\frac{\partial\,[\rho(\varepsilon,t)g(\varepsilon,t)]}{\partial t}\right|_{\text{replenishment}} = \Gamma\rho_0(\varepsilon-\mu(t))g_T(\varepsilon-\mu(t)), \tag{2}$$

where $\rho_0(\varepsilon)$ is the density of states in the absence of a condensate, $g_T(\varepsilon)$ is the Bose-Einstein distribution at temperature T, and Γ is a rate constant such that

$$\Gamma\int_0^\infty \rho_0(\varepsilon)g_T(\varepsilon)\,d\varepsilon = \Phi, \tag{3}$$

where Φ is the flux of atoms from the source *before* evaporation.

2. Three-body loss

The three-body loss term is derived from the master equation term

$$\left.\frac{d\hat{\rho}}{dt}\right|_{3-\text{body loss}} = \frac{1}{3}L_3\int d\boldsymbol{x}\,\mathcal{D}[\hat{\Psi}^3(\boldsymbol{x})]\hat{\rho}, \tag{4}$$

where $\mathcal{D}[\hat{\Psi}]$ is the decoherence superoperator and L_3 is the three-body recombination loss rate constant. A full derivation of the three-body loss terms in Eq. (1) is given in the Appendix.

3. The collisional processes

The collisional "thermal-thermal," "thermal-condensate," and "redistribution" terms in Eq. (1) are identical to those in previous quantum kinetic theory models and are given in the Appendix. Derivations of these terms are given in Ref. [13].

4. The outcoupling process

The outcoupling process from the condensate is modeled as a linear loss process with rate constant γ,

$$\left.\frac{dN_0}{dt}\right|_{\text{outcoupling}} = -\gamma N_0. \tag{5}$$

Modeling the outcoupling in this way neglects any outcoupling from thermal modes. This is a reasonable approximation if focused Raman lasers are used for the outcoupling, which only intersect in the immediate vicinity of the condensate.

IV. RESULTS

The model is fully defined for a given trap geometry by (i) the flux of replenishment atoms, Φ, (ii) the temperature T of those atoms, (iii) the energy of the evaporative cut, ε_{cut}, and (iv) the outcoupling rate from the condensate γ. This section presents the results of the kinetic model for some "typical" parameter values and examines the dependence of the model on each of the parameters.

Our numerical simulations are based on a trap and conditions similar to that of Ref. [18], where a cloud of ^{87}Rb atoms was precooled to an initial temperature slightly greater than the critical temperature before evaporative cooling to study condensate growth. The trap in the experiment was

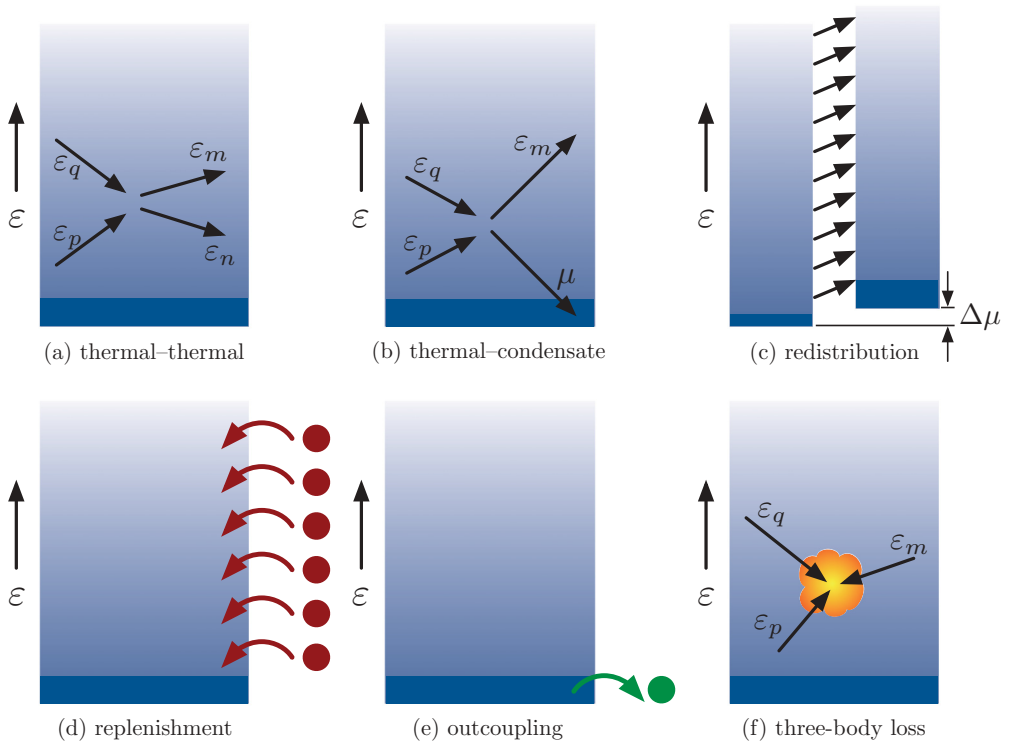

FIG. 2. (Color online) Schematic of processes involved in the evolution of the kinetic model described by (1): collisional processes involving (a) two thermal atoms and (b) one thermal and one condensate atom; (c) the change in the energy distribution function $g(\varepsilon,t)$ if the condensate occupation (and hence chemical potential) increases, raising the energies of every energy level; (d) the replenishment of the thermal cloud from an atomic reservoir; (e) outcoupling from the condensate mode to produce the atom laser; and (f) the loss of atoms due to three-body recombination. The upper shaded rectangle in each panel represents the energy distribution function $g(\varepsilon,t)$ of the thermal cloud, and the bottom dark blue rectangle represents the condensate with occupancy $N_0(t)$ and chemical potential $\varepsilon = \mu(t)$.

axially symmetric with radial and axial trapping frequencies of $\omega_r = 2\pi \times 110$ Hz and $\omega_z = 2\pi \times 14$ Hz, respectively.

To solve the kinetic model numerically, Eq. (1) is discretized along the energy dimension and the resulting coupled differential equations are solved with an adaptive fourth- and fifth-order Runge-Kutta [26] method. Our results are mainly concerned with the steady state of the kinetic model, which we define as being reached when the condensate number has changed by less than 0.1% or 1 atom in 100 ms. The initial state for the simulation is chosen to be a truncated Bose-Einstein distribution containing (before truncation) $N_{\text{initial}} = 4.2 \times 10^6$ atoms at the same temperature as the replenishment reservoir. This state is chosen as a representation of the steady state of the system prior to evaporation. In the trap considered, the critical temperature for 4.2×10^6 atoms is $T_c = 400$ nK.

A. Typical results and parameter studies

As a depiction of the typical time dependence of the results obtained from the kinetic theory model (1), we consider the case in which the thermal cloud is continuously replenished by a source that delivers the initial number of atoms, $N_{\text{initial}} = 4.2 \times 10^6$, to the system once every 5 s. The flux of this source is $\Phi = 8.4 \times 10^5$ atoms/s. The temperature of the replenishment source is chosen to be $T = 540$ nK, 60% above the condensation temperature of the system before evaporation. For the remaining model parameters, we choose the evaporative cutoff to be $\varepsilon_{\text{cut}} = 3k_B T$, and the outcoupling rate from the condensate to be $\gamma = 0.3\ \text{s}^{-1}$.

Figure 3 illustrates the results of the simulation of this system. Figure 3(a) shows the energy distribution of the thermal cloud cooling from the initial truncated Bose-Einstein distribution to a distribution with a lower average energy per particle. Figure 3(b) demonstrates that despite pumping the system with an atomic reservoir above critical temperature it is possible to reach a steady state in which the condensate is macroscopically occupied. In this example the steady-state condensate fraction is 33%.

The nonequilibrium dynamics of the system is not the subject of investigation here; instead our interest is in the steady state itself and in determining the feasibility of creating a pumped atom laser driven by a noncondensed atomic source. As a first step towards this investigation we consider the dependence of the steady-state condensate number on the parameters of the system: Φ, T, ε_{cut}, and γ. The results of this parameter study are presented in Fig. 4, where we use the initial conditions of Fig. 3.

In general the parameter dependencies depicted in Fig. 4 are straightforward; adjusting each parameter causes a monotonic change in the steady-state condensate number. Increasing the flux of atoms to the system increases the steady-state condensate number [Fig. 4(a)], while increasing the temperature of the replenishment source or increasing the outcoupling rate reduces the steady-state condensate number [Figs. 4(b) and 4(c),

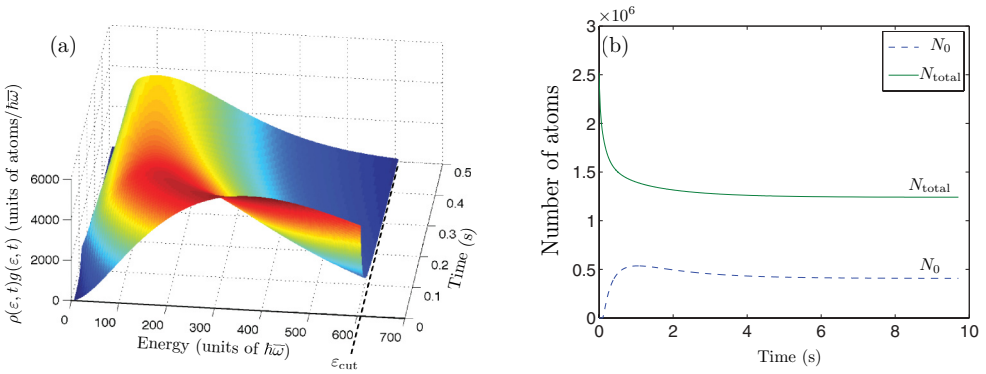

FIG. 3. (Color online) Results of the kinetic model for $\Phi = 8.4 \times 10^5$ atoms/s, $T = 540$ nK, $\varepsilon_{\rm cut} = 3k_BT \approx 610\hbar\overline{\omega}$, and $\gamma = 0.3$ s^{-1}: (a) dynamics of the occupation of the thermal energy levels for $t < 0.5$ s, and (b) the achievement of a steady state of the total and condensed atom numbers over ~10 s. The energy distribution at $t = 0$ is a truncated Bose-Einstein distribution containing (before truncation) $N = 4.2 \times 10^6$ atoms at $T = 540$ nK.

respectively]. The only behavior that is not straightforward is that of Fig. 4(d) in which the dependence on the evaporative cutoff $\varepsilon_{\rm cut}$ is illustrated. For large $\varepsilon_{\rm cut}$, few atoms are lost due to evaporation and the system reaches steady state when the flux of atoms into the system is balanced by three-body and outcoupling losses. As $\varepsilon_{\rm cut}$ is reduced, more atoms are lost due to evaporation and the mean energy per particle reduces, causing the condensate size to increase. As $\varepsilon_{\rm cut}$ continues to decrease, an increasing fraction of the replenishment atoms have an energy greater than $\varepsilon_{\rm cut}$, causing a lower effective atomic flux to be delivered to the system, thereby reducing the steady-state size of any condensate formed. These two competing effects are the origin of the existence of an optimum steady-state condensate number as a function of $\varepsilon_{\rm cut}$ in Fig. 4(d).

As discussed earlier, in the absence of three-body loss the steady-state condensate number would continue to increase as $\varepsilon_{\rm cut}$ is increased. This is because increasing the total number of atoms in the trap at a fixed temperature can only increase the condensate fraction for a fixed rate of outcoupling. It is only because of losses from inelastic collisions and imperfect vacuum systems that it is necessary to evaporate to achieve condensation. This is demonstrated by the dashed line in Fig. 4(d), which asymptotes towards $N_0 = \Phi/\gamma = 2.8 \times 10^6$ atoms in the limit $\varepsilon_{\rm cut} \to \infty$. As observed in the remaining panels of Fig. 4 (in which the effects of three-body loss have been included), the condensate steady state has monotonic dependencies on the source flux, source temperature, and outcoupling rate, which remains true for either the optimum value or a fixed choice of $\varepsilon_{\rm cut}$.

It is now clear that to have the largest steady-state condensate number it is desirable to use a replenishment source with the highest possible flux and the lowest possible temperature. In practice, these two properties are not simultaneously maximized by a single thermal source. A given thermal source achieves a compromise between the two. For example, while a 300-K atomic oven might produce a significantly larger flux than a 50-mK two-dimensional magneto-optical trap (2D MOT), it is not currently possible to create a 50-mK atomic source with the same flux as the 300-K atomic oven. We now examine this trade-off between the temperature and flux in the context of experimentally realizable sources.

B. Behavior in the high-temperature limit

In the previous section we investigated the dependence of the steady-state condensate number on the model parameters. The physical question that we wish to address with this model is: What are the limits of a thermal atom source such that it can realize a pumped, continuous atom laser?

1. Analytical parameter reduction

We now consider the experimentally relevant limit of replenishing the thermal cloud using a high-flux source of thermal atoms. For such sources two simplifications are possible. First, for temperatures greater than T_c the Bose-Einstein energy distribution of the source $g_T(\varepsilon)$ is well approximated by the Boltzmann distribution $g_T(\varepsilon) \approx \zeta e^{-\beta\varepsilon}$ for some constant ζ, and $\beta = (k_BT)^{-1}$. Second, for high-temperature sources the optimum evaporation cutoff $\varepsilon_{\rm cut}$ will be much smaller than the characteristic energy of the source k_BT, and hence $\varepsilon_{\rm cut} \ll k_BT$. From these simplifications it can be seen that the energy distribution below the evaporation cutoff is well described by the single parameter ζ as $g_T(\varepsilon \leqslant \varepsilon_{\rm cut}) \approx \zeta$.

At this point we have rewritten the temperature dependence of the replenishment source in terms of the parameter ζ. However, as the energy distribution of the replenishment source only affects the kinetic model through Eq. (2), its influence on the system dynamics is only through the combined quantity $\kappa = \Gamma\zeta$. An approximate expression for κ in the Boltzmann limit in terms of relevant experimental quantities can be obtained using the definition Eq. (3),

$$\Phi = \Gamma \int_0^\infty \rho_0(\varepsilon) g_T(\varepsilon)\, d\varepsilon \tag{6}$$

$$= \Gamma \int_0^\infty \frac{\varepsilon^2}{2(\hbar\overline{\omega})^3} \zeta e^{-\beta\varepsilon}\, d\varepsilon \tag{7}$$

$$= \Gamma\zeta \frac{1}{2(\hbar\overline{\omega})^3} \int_0^\infty \varepsilon^2 e^{-\beta\varepsilon}\, d\varepsilon \tag{8}$$

$$= \left(\frac{k_BT}{\hbar\overline{\omega}}\right)^3 \Gamma\zeta, \tag{9}$$

$$\kappa \equiv \Gamma\zeta = \Phi \left(\frac{\hbar\overline{\omega}}{k_BT}\right)^3, \tag{10}$$

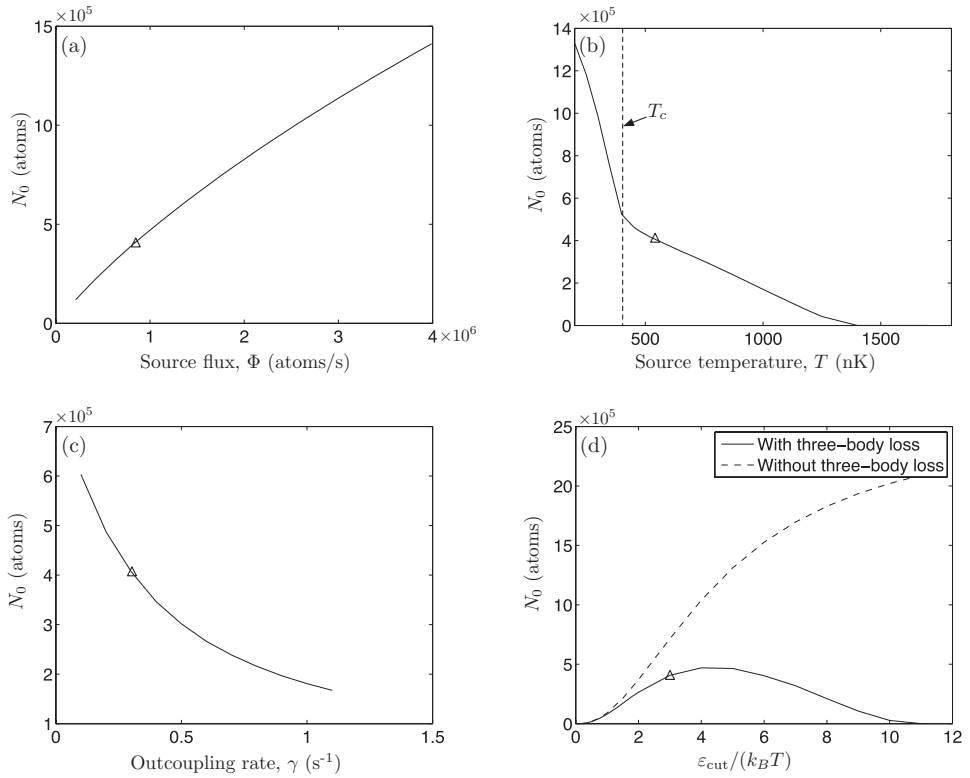

FIG. 4. The dependence of the steady-state condensate number N_0 on the parameters of the quantum kinetic model (1). The steady-state condensate number has a monotonic dependence on (a) the replenishment flux Φ, (b) the temperature T of the replenishment source, and (c) the outcoupling rate γ. For a given choice of the remaining parameters of the model there is (d) an optimum $\varepsilon_{\rm cut}$ for which the steady-state condensate number is a maximum. For each parameter being varied, the remaining parameters are chosen to be the same as for the results depicted in Fig. 3. The triangle in each plot marks the point that corresponds to the precise conditions of Fig. 3 in steady state.

where $\overline{\omega} = (\omega_x\omega_y\omega_z)^{\frac{1}{3}}$ is the geometric mean of the trapping frequencies, and $\rho_0(\varepsilon) = \frac{\varepsilon^2}{2(\hbar\overline{\omega})^3}$ is the density of states in a harmonic trap in the absence of a condensate [22].

We identify κ as the *phase-space flux* of the source as it is directly related to the rate at which the phase-space density of the thermal source is delivered. For a harmonic trap of N thermal atoms at temperature T, the peak phase-space density ϖ is ([22], Chap. 2)

$$\varpi = N\left(\frac{\hbar\overline{\omega}}{k_BT}\right)^3. \tag{11}$$

If these N atoms are delivered over a time τ providing a flux $\Phi = N/\tau$ the peak phase-space flux is

$$\frac{\varpi}{\tau} = \frac{N}{\tau}\left(\frac{\hbar\overline{\omega}}{k_BT}\right)^3 = \Phi\left(\frac{\hbar\overline{\omega}}{k_BT}\right)^3 \equiv \kappa. \tag{12}$$

The parameter ζ is therefore the peak phase-space density ϖ.

The phase-space flux κ is a figure of merit for the thermal source. It quantifies the qualitative behavior already known: for the same atomic flux Φ, a source with a lower temperature will result in a larger condensate [Fig. 4(b)]; and for the same temperature, a source with a higher atomic flux will also result in a larger condensate [Fig. 4(a)]. The phase-space flux also describes exactly how a trade-off between the flux and temperature of the replenishment source will affect the steady-state condensate number. If two sources with different fluxes and temperatures have the same value phase-space flux, then the steady-state condensate number produced by the two sources will be the same (assuming the high-temperature limit applies to both sources). Our interest is in determining what values of κ are necessary to produce a pumped atom laser, and whether such values are presently achievable.

2. *Model parameter scan*

For the limit of high-temperature atomic sources, we have reduced the four variables (Φ, T, $\varepsilon_{\rm cut}$, and γ) required to define the model (1) down to three (κ, $\varepsilon_{\rm cut}$, and γ). Of these three, our main interest is in the dependence of the system on the properties of the atomic source through κ. In contrast, the dependence of the steady-state condensate number on the outcoupling rate γ is simple [see Fig. 4(c)] and the results would not be expected to change qualitatively with γ. It is therefore appropriate to choose a representative value for the outcoupling rate (here $\gamma = 0.3\ {\rm s}^{-1}$) and focus on the remaining two quantities.

As discussed in the previous section there is an optimal choice for the evaporative cutoff $\varepsilon_{\rm cut}$. Our interest here is in the best-case scenario: for a given thermal source, what is the largest condensate we can produce? To examine this question and to verify that κ does fully describe the properties of the thermal source in the high-temperature limit we have performed a parameter scan of the model (1) for a range of fluxes $1.3 \times 10^5\ {\rm s}^{-1} < \Phi < 5 \times 10^{10}\ {\rm s}^{-1}$ and temperatures

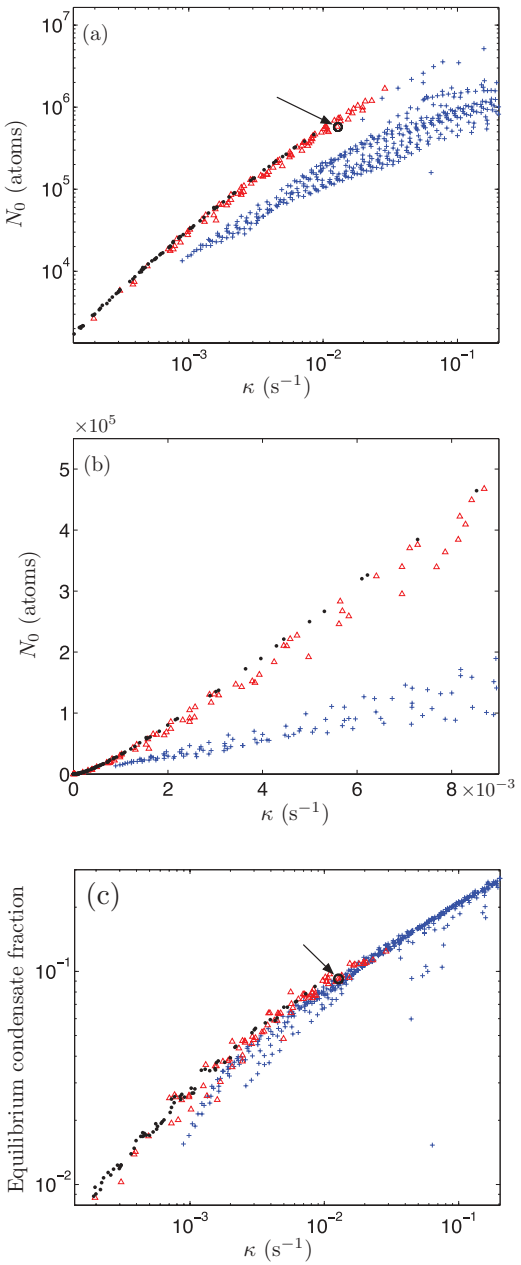

FIG. 5. (Color online) Steady-state condensate properties as a function of the phase-space flux κ for the replenishment source: steady-state condensate number on (a) linear-linear and (b) log-log scales, and (c) steady-state condensate fraction N_0/N. The results of the parameter scan are divided into three groups (black circles, red triangles, and blue crosses) based on their proximity to the high-temperature limit, where κ is expected to be the only figure of merit. The circled point with the arrow pointing to it corresponds to a simulation of the parameters for the last source in Table I, which has $\kappa = 1.1 \times 10^{-2}$ s^{-1} (see main text).

200 nK $< T <$ 600 μK of the atomic source, for each combination determining the optimum evaporative cut $\varepsilon_{\rm cut}$ to give the largest steady-state condensate number. The results of this parameter scan are displayed in Fig. 5 and are separated into three groups based on the ratio $\varepsilon_{\rm cut}/(k_B T)$.

The first group (black circles) have $\varepsilon_{\rm cut}/(k_B T) < 0.1$ and correspond to the high-temperature limit, i.e., $\varepsilon_{\rm cut} \ll k_B T$. Here κ completely determines the properties of the replenishment source. For this group of results, any steady-state property of the system should appear to be a single (not necessarily straight) line when plotted as a function of κ. The results in Fig. 5 demonstrate that these results can be viewed as a single function of κ.

The second group (red triangles) has $0.1 \leqslant \varepsilon_{\rm cut}/(k_B T) < 0.5$ and can be considered to be the results for which the high-temperature limit is a moderate approximation. These results are reasonably close to the results of the first group; however, there is a greater deviation for a given value of κ, indicating that the results can be almost seen as purely a function of κ.

All remaining results fall into the third group (blue crosses) for which $\varepsilon_{\rm cut}/(k_B T) \geqslant 0.5$. It can be seen that these points correspond to a broad range of steady states, indicating that the replenishment source cannot be described by κ alone.

Figures 5(a) and 5(b) both display the steady-state condensate number as a function of the phase-space flux κ. Figure 5(a) uses a log-log scale to highlight the behavior for small and large values of κ, while Fig. 5(b) uses a linear-linear scale to demonstrate that the black circles lying on a single line in Fig. 5(a) are not an artifact of plotting the results using a logarithmic scale. Finally, Fig. 5(c) displays the steady-state condensate fraction as a function of κ.

Figures 5(a) and 5(b) demonstrate that it would be possible to produce atom lasers with condensate numbers $N_0 \gtrsim 10^5$ (corresponding to atom laser fluxes of $\gtrsim 3 \times 10^4$ atoms/s for the outcoupling rate $\gamma = 0.3$ s^{-1} chosen) by using replenishment sources that have a phase-space flux $\kappa \gtrsim 10^{-3}$ s^{-1}. To determine if this is experimentally feasible, the properties of a range of experimental atomic sources are detailed in Table I and the corresponding values of the phase-space flux κ calculated.

The first source listed in Table I is the experiment of Ref. [6] that merged independently produced BECs in optical dipole traps that was discussed previously. This experiment has been included for comparison purposes although not in the high-temperature limit. Of the remaining sources listed in Table I, most are many orders of magnitude away from being useful potential sources for a pumped atom laser (cf. Fig. 5). The fluxes obtainable from these sources are insufficient to compensate for their higher temperatures as an increase of three orders of magnitude in flux is necessary to compensate for an increase of a single order of magnitude in temperature [see Eq. (10)]. Only the last atomic source satisfies the requirement $\kappa \gtrsim 10^{-3}$ s^{-1}. This experiment by Müller *et al.* [7] is one of the sources in a dual atom interferometer designed for the precision measurement of accelerations and rotations [33]. A direct simulation has been performed for the parameters of this source, and the results are marked by a circle with an arrow pointing to it in Fig. 5.

The steady-state condensate number for the source of Müller *et al.* [7] is $N_0 = 5 \times 10^5$ atoms, which would be a sufficiently large condensate to serve as a stable phase reference for an atom laser if it was a pure BEC at zero temperature. However, the steady-state condensate fraction for this source is only 10% [see Fig. 5(c)]; i.e., the thermal cloud contains $N \approx 5 \times 10^6$ atoms.

Previous theoretical work investigating the transfer of statistics from a trapped quasicondensate to an atom laser

TABLE I. Relevant properties of selected experimental cold atomic sources. The phase-space flux κ is evaluated from the atomic flux and temperature values listed using Eq. (10).

Atomic source	Atomic flux Φ	Temperature T	Phase-space flux κ	Reference
BECs in dipole traps	10^5 s^{-1} (55 mHz)[a,b]	<1 μK	$>1.9 \times 10^{-3}$ s^{-1}	[6]
2D$^+$ MOT	9×10^9 s^{-1}	38 mk[c,d]	3×10^{-12} s^{-1}	[27]
2D$^+$ MOT	2×10^{10} s^{-1}	42 mK[c,d]	5×10^{-12} s^{-1}	[28]
MM MOT	10^9 s^{-1}	61 μK[c]	8×10^{-5} s^{-1}	[29]
LVIS	5×10^9 s^{-1}	25 mK[c,d]	6×10^{-12} s^{-1}	[30]
Zeeman slower	3.2×10^{12} s^{-1}	32 mK[c,d]	2×10^{-9} s^{-1}	[31]
Magnetic guide loaded from 3D MOT	7×10^9 s^{-1}	400 μK[c]	2×10^{-6} s^{-1}	[8]
3D MOT loaded from Zeeman slower	2×10^{10} s^{-1} (0.5 Hz)[a]	500 μK	3×10^{-6} s^{-1}	[32]
3D MOT loaded from 2D$^+$ MOT	3×10^8 s^{-1} (3 Hz)[a]	8 μK	1.1×10^{-2} s^{-1}	[7]

[a]This source is pulsed, and the flux is the mean flux over one cycle with the repetition rate listed in parentheses.
[b]This repetition rate is too low for this source to be useful (see main text). It is listed for purposes of comparison only.
[c]In keeping with the best-case scenario investigation being performed, this temperature assumes that the mean velocity of the atoms can be reduced to zero without affecting the distribution. This could be achieved, for example, by firing the source vertically below the main pumped atom laser experiment and taking the atoms from the mean turning point.
[d]The dominant contribution to this temperature is the spread in the longitudinal velocities of the atoms.

found that using high-momentum-kick Raman outcoupling such as that proposed in the scheme presented here can filter some of these fluctuations, resulting in the atom laser having a larger coherence length than the condensate from which it was produced [34].

It is not possible to investigate the transfer of statistics from the trapped component to the atom laser within the present model due to the simplifying assumption that it is only the condensate mode that is outcoupled to form the atom laser. A more detailed three-dimensional model taking into account the full spatial dependence of the Raman outcoupling process would be necessary to fully determine the feasibility of using an atomic source such as that described by Müller *et al*. [7] in the production of a truly continuous pumped atom laser.

V. CONCLUSIONS AND OUTLOOK

We have investigated the feasibility of producing a continuously pumped atom laser fed by evaporation and replenishment with a thermal source. The method has been to investigate the best-case scenario in which the replenishment process introduces no heating to the trapped thermal component beyond that due to bringing the replenishing atoms into contact with the thermal cloud. With these caveats in mind, the results are promising: using an existing experimental source [7] it appears possible to produce steady-state condensates with large atom number ($\sim 5 \times 10^5$ atoms) using the scheme presented in Fig. 1. If the atomic flux of this source could be increased by an order of magnitude, the condensate number produced by this scheme would be pushed to 5×10^6 atoms.

Ultimately it is not the size of the condensate that we are interested in, but the resulting flux of the atom laser and its coherence length. The former goal will certainly be improved by larger steady-state condensate sizes; however, the atom laser must have a sufficiently large coherence length to be useful. It is not clear from the present work whether the coherence length of an atom laser produced using the atomic source of Müller *et al*. [7] will be significantly reduced by the surrounding thermal cloud, although theoretical work [34] suggests this may not occur. To investigate this point it will be necessary to include the full spatial dependence of the Raman outcoupler. This could be achieved by making use of a finite-temperature classical field theory [35].

The results of this work imply that the replenishment source for a collisionally pumped atom laser must be close to degeneracy. The higher flux of higher-temperature thermal atomic sources does not sufficiently compensate for their reduced phase-space density.

ACKNOWLEDGMENTS

This research was supported by the Australian Research Council Centre of Excellence for Quantum-Atom Optics (ACQAO). We acknowledge the use of CPU time at the National Computational Infrastructure National Facility.

APPENDIX: DETAILS OF THE QUANTUM KINETIC THEORY MODEL

One of the difficulties involved in solving the kinetic model is that the energy range that the problem is defined over changes in time. The maximum energy is the energy of the evaporative cutoff $\varepsilon_{\rm cut}$, while the minimum energy is the chemical potential of the condensate, $\mu(t)$. A discretization of the energy dimension over the range $[0,\varepsilon_{\rm cut}]$ will suffer from problems accurately representing the lower end of the distribution where the minimum energy of the thermal atoms is varying.

An alternative method is to write the problem in terms of a shifted energy coordinate $\overline{\varepsilon} \equiv \varepsilon - \mu(t)$ so that the minimum energy of the system is now fixed [13]. A similar problem now occurs at the upper end of the energy range where the maximum energy $\overline{\varepsilon}_{\rm max} = \varepsilon_{\rm cut} - \mu(t)$ is now time dependent. However, at steady state there will be significantly fewer thermal atoms at the evaporation cutoff than there will be near

the condensate [this is illustrated in Fig. 3(a)]. This choice will then result in smaller numerical errors than the alternative.

Written in terms of the shifted energy variable $\overline{\varepsilon}$, the contribution due to the replenishment is

$$\left.\frac{\partial\,[\overline{\rho}(\overline{\varepsilon},t)\overline{g}(\overline{\varepsilon},t)]}{\partial t}\right|_{\text{replenishment}} = \Gamma\overline{\rho}_0(\overline{\varepsilon})\overline{g}_T(\overline{\varepsilon}), \tag{A1}$$

where a bar over a function is used to indicate that it is defined in terms of the shifted energy coordinate. The original form of this term is given by Eq. (2).

1. Density of states

The density of states for the thermal cloud is modified from its form in a harmonic trap due to the mean-field repulsion of the condensate mode. The effective potential experienced by the thermal atoms is

$$V_{\text{eff}}(\boldsymbol{r},t) = V_{\text{trap}}(\boldsymbol{r}) + 2gn_c(\boldsymbol{r},t), \tag{A2}$$

where $V_{\text{trap}}(\boldsymbol{r})$ is the potential due to the magnetic trap, $g = 4\pi\hbar^2 a/m$, a is the s-wave scattering length, and $n_c(\boldsymbol{r},t)$ is the condensate density which was assumed to follow a Thomas-Fermi distribution. Note that the "2" in the above expression is the full Hartree-Fock mean field experienced by the thermal atoms (see Chap. 8 of Ref. [22] for further details) which is twice the mean-field repulsion experienced by condensate atoms.

The density of states in the presence of the effective potential (A2) is given by

$$\rho(\varepsilon,t) = \int \frac{d\boldsymbol{r}\,d\boldsymbol{p}}{(2\pi\hbar)^3}\,\delta(\varepsilon - V_{\text{eff}}(\boldsymbol{r},t) - \boldsymbol{p}^2/2m). \tag{A3}$$

The integrals are performed in Ref. [13] giving the following result in terms of the shifted energy coordinate (Eqs. (49) and (50) in Ref. [13]):

$$\overline{\rho}(\overline{\varepsilon},t) = \frac{2}{\pi\hbar\overline{\omega}}\left[I_-(\overline{\varepsilon}) + I_+(\overline{\varepsilon})\right], \tag{A4}$$

where the functions $I_\pm(\overline{\varepsilon})$ are

$$I_-(\overline{\varepsilon}) = \frac{u_-^3 x}{4} - \frac{a_- u_- x}{8} - \frac{a_-^2}{8}\ln(x+u_-)\Big|_{x=\sqrt{\max\{0,-a_-\}}}^{x=\sqrt{2\mu/\hbar\overline{\omega}}}, \tag{A5}$$

$$I_+(\overline{\varepsilon}) = -\frac{u_+^3 x}{4} + \frac{a_+ u_+ x}{8} + \frac{a_+^2}{8}\arcsin\left(\frac{x}{\sqrt{a_+}}\right)\Big|_{x=\sqrt{2\mu/\hbar\overline{\omega}}}^{x=\sqrt{a_+}}, \tag{A6}$$

with $a_\pm = 2(\overline{\varepsilon}\pm\mu)/\hbar\overline{\omega}$, and $u_\pm = \sqrt{a_\pm \mp x^2}$.[1]

2. Collision and energy redistribution in quantum kinetic theory

A full derivation of the forms of the collision and energy-redistribution terms of the kinetic model is given in Refs. [13,25]. The contribution due to thermal-thermal collisions is given in Eq. (26) of Ref. [13] and has the form

$$\begin{aligned}\left.\frac{\partial\,[\overline{\rho}(\overline{\varepsilon}_1,t)\overline{g}(\overline{\varepsilon}_1,t)]}{\partial t}\right|_{\text{thermal}-\text{thermal}} &= \frac{m^3g^2}{2\pi^3\hbar^7}\int d\overline{\varepsilon}_2\int d\overline{\varepsilon}_3\int d\overline{\varepsilon}_4\,\overline{\rho}(\overline{\varepsilon}_{\min},t)\\ &\times\delta(\overline{\varepsilon}_1+\overline{\varepsilon}_2-\overline{\varepsilon}_3-\overline{\varepsilon}_4)\\ &\times[(1+\overline{g}_1)(1+\overline{g}_2)\overline{g}_3\overline{g}_4 - \overline{g}_1\overline{g}_2(1+\overline{g}_3)(1+\overline{g}_4)],\end{aligned} \tag{A7}$$

where $\overline{\varepsilon}_{\min}$ is the minimum of the $\overline{\varepsilon}_i$, and $\overline{g}_i = \overline{g}(\overline{\varepsilon}_i,t)$.

The contribution due to thermal-condensate collisions is given by Eqs. (53) and (58)–(60) of Ref. [13] and has the form

$$\begin{aligned}\left.\frac{\partial\,[\overline{\rho}(\overline{\varepsilon}_1,t)\overline{g}(\overline{\varepsilon}_1,t)]}{\partial t}\right|_{\text{thermal}-\text{condensate}} &= \frac{m^3g^2}{2\pi^3\hbar^7}\int d\overline{\varepsilon}_2\int d\overline{\varepsilon}_3\int d\overline{\varepsilon}_4\,\delta(\overline{\varepsilon}_2-\overline{\varepsilon}_3-\overline{\varepsilon}_4)\\ &\times[\delta(\overline{\varepsilon}_1-\overline{\varepsilon}_2)-\delta(\overline{\varepsilon}_1-\overline{\varepsilon}_3)-\delta(\overline{\varepsilon}_1-\overline{\varepsilon}_4)]\\ &\times[(1+\overline{g}_2)\overline{g}_3\overline{g}_4 - \overline{g}_2(1+\overline{g}_3)(1+\overline{g}_4)]\\ &\times\int_{\overline{U}_{\text{eff}}(\boldsymbol{r},t)\leqslant\overline{U}_-} d\boldsymbol{r}\,n_c(\boldsymbol{r},t),\end{aligned} \tag{A8}$$

where $\overline{U}_- = \frac{2}{3}[(\overline{\varepsilon}_3+\overline{\varepsilon}_4) - \sqrt{\overline{\varepsilon}_3^2 - \overline{\varepsilon}_3\overline{\varepsilon}_4 + \overline{\varepsilon}_4^2}]$, and $\overline{U}_{\text{eff}}(\boldsymbol{r},t) = U_{\text{eff}}(\boldsymbol{r},t) - \mu(t)$. The corresponding contribution to the evolution of the condensate number is

$$\left.\frac{dN_0}{dt}\right|_{\text{thermal}-\text{condensate}} = -\int d\overline{\varepsilon}\,\left.\frac{\partial\,[\overline{\rho}(\overline{\varepsilon},t)\overline{g}(\overline{\varepsilon},t)]}{\partial t}\right|_{\text{thermal}-\text{condensate}}. \tag{A9}$$

Finally, the contribution due to energy redistribution is (Eqs. (32) and (52) in Ref. [13])

$$\left.\frac{\partial\,[\overline{\rho}(\overline{\varepsilon}_1,t)\overline{g}(\overline{\varepsilon}_1,t)]}{\partial t}\right|_{\text{redistribution}} = -\frac{\partial(\overline{\rho}_{\text{w}}\overline{g})}{\partial\overline{\varepsilon}}, \tag{A10}$$

where $\overline{\rho}_{\text{w}}$ is the weighted density of states

$$\overline{\rho}_{\text{w}}(\overline{\varepsilon}) = \frac{2}{\pi\hbar\overline{\omega}}\left[I_-(\overline{\varepsilon}) - I_+(\overline{\varepsilon})\right]\frac{d\mu}{dt}, \tag{A11}$$

where the functions $I_\pm(\overline{\varepsilon})$ are given in Eqs. (A5) and (A6).

3. Three-body loss in quantum kinetic theory

The dominant density-dependent loss process in Bose-Einstein condensates is three-body loss [36,37]. Three-body loss (or three-body recombination) is the process in which three atoms collide, forming a bound dimer with the third atom necessary to ensure both energy and momentum conservation. The binding energy is sufficient to give the products of a three-body recombination process sufficient kinetic energy to rapidly escape the trap. Three-body loss is then well described by the master equation term

$$\left.\frac{d\hat{\rho}}{dt}\right|_{3-\text{body loss}} = \frac{1}{3}L_3\int d\boldsymbol{x}\,\mathcal{D}[\hat{\Psi}^3(\boldsymbol{x})]\hat{\rho}, \tag{A12}$$

[1] There is a minor typographical error in Bijlsma *et al.* [13]: the lower limit of $I_-(\overline{\varepsilon})$ is given as $x = \sqrt{\max\{0,a_-\}}$, whereas it should read $x = \sqrt{\max\{0,-a_-\}}$ as in Eq. (A5).

where $\mathcal{D}[\hat{c}]\hat{\rho} = \hat{c}\hat{\rho}\hat{c}^\dagger - \frac{1}{2}(\hat{c}^\dagger\hat{c}\hat{\rho} + \hat{\rho}\hat{c}^\dagger\hat{c})$ is the decoherence superoperator, and $L_3 = 5.8 \times 10^{-30}\ \mathrm{cm^6 s^{-1}}$ [36] is the three-body recombination loss rate constant. This equation, first derived in Ref. [38], has the familiar form of a decoherence superoperator with the state undergoing loss as the argument.

The loss rate of atoms from the system due to three-body loss is readily obtained from Eq. (A12) as

$$\left.\frac{dN}{dt}\right|_{3-\text{body loss}} = \mathrm{Tr}\left\{\int d\boldsymbol{r}\ \hat{\Psi}^\dagger(\boldsymbol{r})\hat{\Psi}(\boldsymbol{r})\left.\frac{d\hat{\rho}}{dt}\right|_{3-\text{body loss}}\right\} = -L_3\int d\boldsymbol{r}\ \langle\hat{\Psi}^\dagger(\boldsymbol{r})^3\hat{\Psi}(\boldsymbol{r})^3\rangle. \tag{A13}$$

To separate the contributions to Eq. (A13) due to the thermal and condensed components, we use a broken-symmetry approach. We write the annihilation operator $\hat{\Psi}$ in terms of its mean value $\Psi \equiv \langle\hat{\Psi}\rangle$ and the fluctuation operator $\delta\hat{\Psi} \equiv \hat{\Psi} - \Psi$ and substitute this into Eq. (A13). The fluctuation operator defined here includes thermal fluctuations, which cannot be considered to be small. Higher powers of $\delta\hat{\Psi}$ can therefore not be neglected. However, thermal fluctuations have no well-defined phase relationship to one another or to the condensate. Expectation values containing an unequal number of creation and annihilation deviation operators such as $(\delta\hat{\Psi}\delta\hat{\Psi})$ can therefore be assumed to be zero.

Performing the substitution described, Eq. (A13) becomes

$$\begin{aligned}\left.\frac{dN}{dt}\right|_{3-\text{body loss}} &= -L_3\int d\boldsymbol{r}\ \{[n_c(\boldsymbol{r})]^3 + 9[n_c(\boldsymbol{r})]^2\langle\delta\hat{\Psi}^\dagger(\boldsymbol{r})\delta\hat{\Psi}(\boldsymbol{r})\rangle \\ &\quad + 9n_c(\boldsymbol{r})\langle\delta\hat{\Psi}^\dagger(\boldsymbol{r})^2\delta\hat{\Psi}(\boldsymbol{r})^2\rangle + \langle\delta\hat{\Psi}^\dagger(\boldsymbol{r})^3\delta\hat{\Psi}(\boldsymbol{r})^3\rangle\},\end{aligned} \tag{A14}$$

where $n_c(\boldsymbol{r}) = |\Psi(\boldsymbol{r})|^2$ is the condensate density.

The noncondensate density is given by $n_T(\boldsymbol{r}) = \langle\delta\hat{\Psi}^\dagger(\boldsymbol{r})\delta\hat{\Psi}(\boldsymbol{r})\rangle$. As thermal states are Gaussian, the higher-order expectation values in the previous expression may be simplified by the application of Wick's theorem [39], giving

$$\langle\delta\hat{\Psi}^\dagger(\boldsymbol{r})^2\delta\hat{\Psi}(\boldsymbol{r})^2\rangle = 2[n_T(\boldsymbol{r})]^2, \tag{A15}$$

$$\langle\delta\hat{\Psi}^\dagger(\boldsymbol{r})^3\delta\hat{\Psi}(\boldsymbol{r})^3\rangle = 6[n_T(\boldsymbol{r})]^3. \tag{A16}$$

Substituting these expressions back into Eq. (A14) yields

$$\left.\frac{dN}{dt}\right|_{3-\text{body loss}} = -L_3\int d\boldsymbol{r}\ [n_c(\boldsymbol{r})]^3 + 9[n_c(\boldsymbol{r})]^2 n_T(\boldsymbol{r}) + 18n_c(\boldsymbol{r})[n_T(\boldsymbol{r})]^2 + 6[n_T(\boldsymbol{r})]^3. \tag{A17}$$

The evaluation of this loss rate requires the evaluation of the condensate and thermal densities. The condensate density $n_c(\boldsymbol{r})$ is fully determined by the condensate occupation $N_0(t)$ within the Thomas-Fermi approximation that has already been made elsewhere in the derivation of the kinetic model. The first term of Eq. (A17) only involves the condensate density and may be evaluated analytically:

$$\frac{dN_0}{dt} = -L_3\frac{15^{4/5}}{168\pi^2}\left(\frac{m\bar{\omega}}{\hbar\sqrt{a}}\right)^{12/5}N_0^{9/5}. \tag{A18}$$

The remaining terms of Eq. (A17) require an expression for the thermal density $n_T(\boldsymbol{r})$, which can be obtained from the energy distribution function $g(\varepsilon)$ and the density of states, $\rho(\varepsilon)$.

The total number of thermal atoms, N_T, can be written as

$$N_T = \int d\varepsilon\ \rho(\varepsilon)g(\varepsilon), \tag{A19}$$

where the density of states is defined by Eq. (A3). Substituting this into Eq. (A19) and rearranging the order of integrals gives

$$N_T = \int d\boldsymbol{r}\int d\varepsilon\ \rho(\varepsilon,\boldsymbol{r})g(\varepsilon), \tag{A20}$$

where we have defined

$$\rho(\varepsilon,\boldsymbol{r}) = \int d\boldsymbol{p}\,\delta(\varepsilon - V_{\text{eff}}(\boldsymbol{r},t) - \boldsymbol{p}^2/2m) = \frac{m^{3/2}}{\sqrt{2}\pi^2\hbar^3}\sqrt{\varepsilon - V_{\text{eff}}(\boldsymbol{r})}. \tag{A21}$$

The thermal density can be identified from Eq. (A20):

$$n_T(\boldsymbol{r}) = \int d\varepsilon\ \rho(\varepsilon,\boldsymbol{r})g(\varepsilon). \tag{A22}$$

The remaining terms of Eq. (A17) can now be expressed in terms of the energy distribution function $g(\varepsilon)$ and the density of states, $\rho(\varepsilon)$, by substituting Eq. (A22) for one of the factors of $n_T(\boldsymbol{r})$ in each term:

$$-L_3\int d\boldsymbol{r}\ 9[n_c(\boldsymbol{r})]^2 n_T(\boldsymbol{r}) = -L_3\int d\varepsilon\ g(\varepsilon)\int d\boldsymbol{r}\ 9\rho(\varepsilon,\boldsymbol{r})[n_c(\boldsymbol{r})]^2, \tag{A23}$$

$$-L_3\int d\boldsymbol{r}\ 18n_c(\boldsymbol{r})[n_T(\boldsymbol{r})]^2 = -L_3\int d\varepsilon\ g(\varepsilon)\int d\boldsymbol{r}\ 18\rho(\varepsilon,\boldsymbol{r})n_c(\boldsymbol{r})n_T(\boldsymbol{r}), \tag{A24}$$

$$-L_3\int d\boldsymbol{r}\ 6[n_T(\boldsymbol{r})]^3 = -L_3\int d\varepsilon\ g(\varepsilon)\int d\boldsymbol{r}\ 6\rho(\varepsilon,\boldsymbol{r})[n_T(\boldsymbol{r})]^2. \tag{A25}$$

From these expressions the rate of loss of atoms of energy ε from the distribution can be identified:

$$\left.\frac{\partial\,[\rho(\varepsilon)g(\varepsilon)]}{\partial t}\right|_{3-\text{body loss}} = -L_3\int d\boldsymbol{r}\ \rho(\varepsilon,\boldsymbol{r})g(\varepsilon)\{3[n_c(\boldsymbol{r})]^2 + 12n_c(\boldsymbol{r})n_T(\boldsymbol{r}) + 6[n_T(\boldsymbol{r})]^2\}, \tag{A26}$$

where the contributions due to the terms involving only one or two thermal atoms have been multiplied by 1/3 and 2/3, respectively, to share appropriately the total loss. The corresponding term for the condensate number evolution is

$$\left.\frac{dN_0}{dt}\right|_{3-\text{body loss}} = -L_3\frac{15^{4/5}}{168\pi^2}\left(\frac{m\bar{\omega}}{\hbar\sqrt{a}}\right)^{12/5}N_0^{9/5} - L_3\int d\varepsilon\int d\boldsymbol{r}\ \rho(\varepsilon,\boldsymbol{r})g(\varepsilon)\{6[n_c(\boldsymbol{r})]^2 + 6n_c(\boldsymbol{r})n_T(\boldsymbol{r})\}, \tag{A27}$$

where the contributions due to the terms involving only one or two condensate atoms have been multiplied by 1/3 and 2/3, respectively.

[1] F. Dalfovo *et al*., Rev. Mod. Phys. **71**, 463 (1999); A. J. Leggett, *ibid*. **73**, 307 (2001); M. H. Anderson *et al*., Science **269**, 198 (1995); K. B. Davis, M. O. Mewes, M. R. Andrews, N. J. van Druten, D. S. Durfee, D. M. Kurn, and W. Ketterle, Phys. Rev. Lett. **75**, 3969 (1995); C. C. Bradley, C. A. Sackett, J. J. Tollett, and R. G. Hulet, *ibid*. **75**, 1687 (1995).

[2] H. M. Wiseman, Phys. Rev. A **56**, 2068 (1997).

[3] M.-O. Mewes, M. R. Andrews, D. M. Kurn, D. S. Durfee, C. G. Townsend, and W. Ketterle, Phys. Rev. Lett. **78**, 582 (1997); J.-F. Riou, W. Guerin, Y. Le Coq, M. Fauquembergue, V. Josse, P. Bouyer, and A. Aspect, *ibid*. **96**, 070404 (2006); N. P. Robins, C. Figl, S. A. Haine, A. K. Morrison, M. Jeppesen, J. J. Hope, and J. D. Close, *ibid*. **96**, 140403 (2006); A. Öttl, S. Ritter, M. Köhl, and T. Esslinger, *ibid*. **95**, 090404 (2005).

[4] M. Johnsson, S. Haine, J. J. Hope, N. P. Robins, C. Figl, M. Jeppesen, J. Dugué, and J. D. Close, Phys. Rev. A **75**, 043618 (2007); M. T. Johnsson and J. J. Hope, *ibid*. **75**, 043619 (2007).

[5] L. Mandel and E. Wolf, *Optical Coherence and Quantum Optics* (Cambridge University Press, Cambridge, 1995).

[6] A. P. Chikkatur, Y. Shin, A. E. Leanhardt, D. Kielpinski, E. Tsikata, T. L. Gustavson, D. E. Pritchard, and W. Ketterle, Science **296**, 2193 (2002).

[7] T. Müller, T. Wendrich, M. Gilowski, C. Jentsch, E. M. Rasel, and W. Ertmer, Phys. Rev. A **76**, 063611 (2007).

[8] T. Lahaye, J. M. Vogels, K. J. Günter, Z. Wang, J. Dalibard, and D. Guéry-Odelin, Phys. Rev. Lett. **93**, 093003 (2004).

[9] A. Greiner, J. Sebastian, P. Rehme, A. Aghajani-Talesh, A. Griesmaier, and T. Pfau, J. Phys. B **40**, F77 (2007).

[10] H. M. Wiseman and M. J. Collett, Phys. Lett. A **202**, 246 (1995); S. Bhongale and M. Holland, Phys. Rev. A **62**, 043604 (2000); L. Santos, F. Floegel, T. Pfau, and M. Lewenstein, *ibid*. **63**, 063408 (2001).

[11] N. P. Robins, C. Figl, M. Jeppesen, G. R. Dennis, and J. D. Close, Nat. Phys. **4**, 731 (2008).

[12] M. Falkenau, V. V. Volchkov, J. Rührig, A. Griesmaier, and T. Pfau, Phys. Rev. Lett. **106**, 163002 (2011).

[13] M. J. Bijlsma, E. Zaremba, and H. T. C. Stoof, Phys. Rev. A **62**, 063609 (2000).

[14] C. W. Gardiner and P. Zoller, Phys. Rev. A **55**, 2902 (1997); D. Jaksch, C. W. Gardiner, and P. Zoller, *ibid*. **56**, 575 (1997); C. W. Gardiner and P. Zoller, *ibid*. **58**, 536 (1998); D. Jaksch, C. W. Gardiner, K. M. Gheri, and P. Zoller, *ibid*. **58**, 1450 (1998); C. W. Gardiner and P. Zoller, *ibid*. **61**, 033601 (2000); M. D. Lee and C. W. Gardiner, *ibid*. **62**, 033606 (2000).

[15] M. J. Davis, C. W. Gardiner, and R. J. Ballagh, Phys. Rev. A **62**, 063608 (2000).

[16] C. W. Gardiner, Phys. Rev. A **56**, 1414 (1997).

[17] N. P. Robins, C. Figl, S. A. Haine, A. K. Morrison, M. Jeppesen, J. J. Hope, and J. D. Close, Phys. Rev. Lett. **96**, 140403 (2006).

[18] M. Köhl, M. J. Davis, C. W. Gardiner, T. W. Hänsch, and T. Esslinger, Phys. Rev. Lett. **88**, 080402 (2002).

[19] M. J. Davis and C. W. Gardiner, J. Phys. B **35**, 733 (2002).

[20] M. Hugbart, J. A. Retter, A. F. Varòn, P. Bouyer, A. Aspect, and M. J. Davis, Phys. Rev. A **75**, 011602(R) (2007).

[21] M. C. Garrett, A. Ratnapala, E. D. van Ooijen, C. J. Vale, K. Weegink, S. K. Schnelle, O. Vainio, N. R. Heckenberg, H. Rubinsztein-Dunlop, and M. J. Davis, Phys. Rev. A **83**, 013630 (2011).

[22] C. J. Pethick and H. Smith, *Bose-Einstein Condensation in Dilute Gases* (Cambridge University Press, Cambridge, 2002).

[23] O. J. Luiten, M. W. Reynolds, and J. T. M. Walraven, Phys. Rev. A **53**, 381 (1996).

[24] A. C. J. Wade, D. Baillie, and P. B. Blakie, Phys. Rev. A **84**, 023612 (2011).

[25] N. P. Proukakis and B. Jackson, J. Phys. B **41**, 203002 (2008).

[26] W. H. Press, S. A. Teukolsky, W. T. Vetterling, and B. P. Flannery, *Numerical Recipes*, 3rd ed. (Cambridge University Press, Cambridge, 2007).

[27] K. Dieckmann, R. J. C. Spreeuw, M. Weidemüller, and J. T. M. Walraven, Phys. Rev. A **58**, 3891 (1998).

[28] S. Chaudhuri, S. Roy, and C. S. Unnikrishnan, Phys. Rev. A **74**, 023406 (2006).

[29] P. Cren, C. F. Roos, A. Aclan, J. Dalibard, and D. Guéry-Odelin, Eur. Phys. J. D **20**, 107 (2002).

[30] Z. T. Lu, K. L. Corwin, M. J. Renn, M. H. Anderson, E. A. Cornell, and C. E. Wieman, Phys. Rev. Lett. **77**, 3331 (1996).

[31] C. Slowe, L. Vernac, and L. V. Hau, Rev. Sci. Instrum. **76**, 103101 (2005).

[32] E. W. Streed, A. P. Chikkatur, T. L. Gustavson, M. Boyd, Y. Torii, D. Schneble, G. K. Campbell, D. E. Pritchard, and W. Ketterle, Rev. Sci. Instrum. **77**, 023106 (2006).

[33] T. Müller, M. Gilowski, M. Zaiser, P. Berg, C. Schubert, T. Wendrich, W. Ertmer, and E. M. Rasel, Eur. Phys. J. D **53**, 273 (2009).

[34] N. P. Proukakis, Laser Phys. **13**, 527 (2003).

[35] P. B. Blakie, A. S. Bradley, M. J. Davis, R. J. Ballagh, and C. W. Gardiner, Adv. Phys. **57**, 363 (2008).

[36] E. A. Burt, R. W. Ghrist, C. J. Myatt, M. J. Holland, E. A. Cornell, and C. E. Wieman, Phys. Rev. Lett. **79**, 337 (1997).

[37] J. Söding, D. Guéry-Odelin, P. Desbiolles, F. Chevy, H. Inamori, and J. Dalibard, Appl. Phys. B **69**, 257 (1999).

[38] M. W. Jack, Phys. Rev. Lett. **89**, 140402 (2002).

[39] G. C. Wick, Phys. Rev. **80**, 268 (1950).